

## Noise-induced oscillatory behavior in field-dependent relaxational dynamics

J. Buceta,<sup>1</sup> Kevin Wood,<sup>2,3</sup> and Katja Lindenberg<sup>2</sup>

<sup>1</sup>*Parc Científic de Barcelona, Centre de Recerca en Química Teòrica (CeRQT), Campus Diagonal—Universitat de Barcelona, Edifici Modular, C/Josep Samitier 1-5, 08028 Barcelona, Spain*

<sup>2</sup>*Department of Chemistry and Biochemistry 0340, and Institute for Nonlinear Science, University of California, San Diego, La Jolla, California 92093, USA*

<sup>3</sup>*Department of Physics, University of California, San Diego, La Jolla, California 92093, USA*

(Received 24 November 2005; revised manuscript received 8 February 2006; published 19 April 2006)

By considering inertial effects in a field-dependent relaxational model, we show that noise may induce collective oscillatory dynamics. In agreement with the recently introduced idea of noise-induced multistability, we show that there is a region in parameter space where such behavior depends on the initial condition. Moreover, when the coupling term leads to pattern formation by means of a morphological instability *a la* Swift-Hohenberg, [J. Buceta, M. Ibañes, J. M. Sancho, and K. Lindenberg, Phys. Rev. E **67**, 021113 (2003) and K. Wood, J. Buceta, and K. Lindenberg, Phys. Rev. E **73**, 022101 (2006)] our numerical simulations reveal that spatio-temporal oscillatory structures develop.

DOI: [10.1103/PhysRevE.73.042101](https://doi.org/10.1103/PhysRevE.73.042101)

PACS number(s): 05.40.-a, 05.10.Gg, 64.60.-i

Field-dependent relaxational dynamics has been a subject of considerable recent interest [1–6]. These models provide a mechanism for noise-induced phase transitions that does not require a Stratonovich drift [7,8]. In certain noise intensity regimes these systems may exhibit noise-induced multistability phenomena and the associated hysteresis, such that the system can settle into an ordered or a disordered state depending on the initial condition [9,10]. A comprehensive study has revealed that the occurrence of these features depends only on the balance of convexities between the relaxational parameter and the local potential of the model, and not on the particular form of these functionals [9,10].

Phase transitions induced purely by noise were first noted in extended systems where the transition is induced dynamically in the sense that it arises from a short-time instability of the local dynamics which becomes globally stabilized at longer times by the spatial coupling [2,6]. More recently, noise-induced phase transitions have been found in relaxational systems in which it is possible to obtain a steady-state probability distribution that leads to a nonequilibrium free energy [4,6–10]. Transitions to globally ordered states in such relaxational systems involve nearest neighbor coupling, which in a continuum version translates to diffusive coupling. A modification of the coupling to include more distant neighbors, e.g., one that in a continuum version is represented by a Swift-Hohenberg coupling, extends the noise-induced phenomena to pattern formation [8,10].

Typically, these transitions between disordered and ordered or patterned states have been studied in systems described by a *single* field. The case of *two* coupled fields has been explored recently [11], with the conclusion that macroscopic limit cycles can also be induced via pure noise-induced phase transitions. These studies specifically focused on dynamically induced phase transitions and therefore depend on the Stratonovich drift, i.e., on the interpretation of the noise. In parallel with that idea, herein we consider such behavior in systems where the interpretation of the noise is irrelevant to the occurrence of the phenomenon. Thus, we consider the role of an additional field in a relaxational dynamics with field-dependent coefficients. The additional field

leads to noise-induced collective oscillatory behavior, including oscillatory spatio-temporal structures.

Consider the Langevin equation defined on a lattice

$$\dot{\varphi}_i = -\Gamma(\varphi) \frac{\delta \mathcal{F}(\{\varphi\})}{\delta \varphi_i} + [\Gamma(\varphi_i)]^{1/2} \xi_i(t), \quad (1)$$

where  $\varphi_i$  is a scalar field at site  $i$ ,  $\Gamma(\varphi_i)$  is the field-dependent kinetic coefficient,  $\mathcal{F}(\{\varphi\})$  is an energy functional, and  $\xi_i(t)$  is a spatio-temporal white noise with zero mean and intensity  $\sigma^2$ ,  $\langle \xi_i(t) \xi_j(t') \rangle = \sigma^2 \delta_{ij} \delta(t-t')$ . The interpretation of the noise in this model at most affects quantitative results such as the values of critical parameters but does not affect the occurrence of the phenomena themselves. For convenience, we choose the Itô interpretation.

Equation (1) is the most general description possible for the relaxational dynamics of a scalar field in which a generalized fluctuation-dissipation relation holds. The Lyapunov functional  $\mathcal{F}$  drives the evolution and contains energy contributions from a local potential and an interaction term (surface tension). Here we focus on a harmonic local potential, and first we consider nearest neighbor interactions. Thus  $\mathcal{F}$  reads

$$\mathcal{F}(\{\varphi\}) = \sum_i \left( \frac{\varphi_i^2}{2} + \frac{K}{4d} \sum_{\langle ij \rangle} (\varphi_j - \varphi_i)^2 \right), \quad (2)$$

where  $d$  is the spatial dimension and  $K$  the coupling strength. The inner sum in Eq. (2) runs over the nearest neighbors of site  $i$ , and therefore the interaction corresponds to a discrete version of a squared gradient. Under such conditions, and if the relaxational coefficient is a constant, Eq. (1) is the discrete version of the so-called continuous Gaussian model. It is trivial to see that in that case the model does not show any order-disorder phase transition or other interesting behavior. It simply relaxes toward the homogeneous disordered state  $\{\varphi\}=0$ . However, when the relaxational coefficient depends on the value of the field, Eq. (1) presents a rich phenomenology that ranges from inverted phase diagrams to noise-induced multistability depending on the specific form of

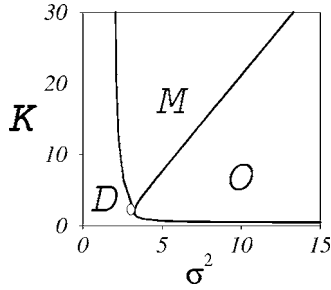


FIG. 1. Phase diagram of Eq. (1) in the parameter space of intensity of the coupling,  $K$ , and intensity of the fluctuations,  $\sigma^2$ . The capital letters  $D$ ,  $O$ , and  $M$  indicate the disordered stable phase ( $\langle\varphi\rangle=0$ ), the ordered stable phase ( $\langle\varphi\rangle\neq 0$ ), and the multistable phase ( $\langle\varphi\rangle=0$  and  $\langle\varphi\rangle\neq 0$  both stable), respectively. The open circle indicates a triple point where all the phases merge. From [9].

$\Gamma(\varphi)$  [9]. In particular, we have shown that the sign of the curvature of  $\Gamma(\varphi)$  around the origin determines the asymptotic stationary phase.

On the basis of a mean field approximation equivalent to a global coupling description, we found the phase diagram shown in Fig. 1 for the spatially and noise averaged field  $\langle\varphi\rangle$ . We assumed a harmonic local potential and the particular choice  $\Gamma(\varphi)=(1+\varphi^2)/(1+\varphi^4)$  as a generic example of a relaxational coefficient with a local minimum at the origin. Note the ordering role of the fluctuations as well as the noise-induced multistability when  $K$  is sufficiently large. That is, there is no ordered phase if the individual oscillators are decoupled from one another and/or if there is no noise.

Consider now the diffusive problem with an additional degree of freedom  $z_i$ ,

$$\begin{aligned} \dot{\varphi}_i &= -\Gamma(\varphi_i)\frac{\delta\mathcal{F}(\{\varphi\})}{\delta\varphi_i} + [\Gamma(\varphi_i)]^{1/2}\xi_i(t) - \omega z_i, \\ \dot{z}_i &= \omega\varphi_i, \end{aligned} \quad (3)$$

where  $\omega$  is a frequency. The system (3) can be expressed as a single equation including an inertial term,  $\ddot{z}_i$ , as

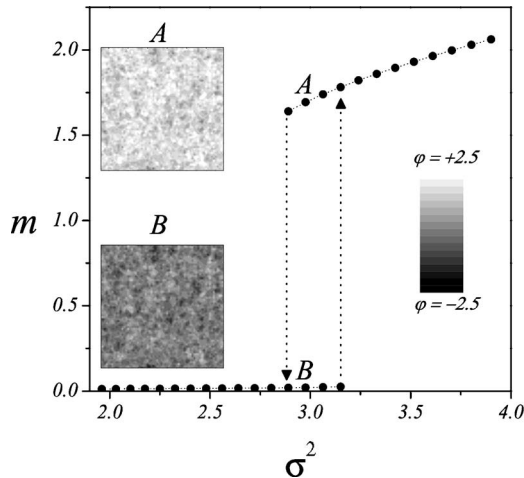


FIG. 2. Order parameter  $m=|\langle\varphi\rangle|$  obtained from numerical simulations of Eq. (1) for  $K=10$  as a function of the intensity of the fluctuations. The insets show a density plot of the field for two different sets of initial conditions and  $\sigma^2\approx 3$ , where the system presents multistability. From [9].

$$\ddot{z}_i + \omega^2 z_i = \omega G(\{\varphi\}), \quad (4)$$

where

$$G(\{\varphi\}) = -\Gamma(\varphi_i)\frac{\delta\mathcal{F}(\{\varphi\})}{\delta\varphi_i} + [\Gamma(\varphi_i)]^{1/2}\xi_i(t). \quad (5)$$

In Eq. (4) it is understood that every  $\varphi_i$  on the right hand side is to be replaced by  $\dot{z}_i/\omega$ ; it is thus a closed second-order stochastic differential equation for the set  $\{z_i\}$ .

The mean field description of the system reads

$$\dot{\varphi} = G(\varphi; \langle\varphi\rangle) - \omega z, \quad \dot{z} = \omega\varphi, \quad (6)$$

where

$$G(\varphi; \langle\varphi\rangle) = -\Gamma(\varphi)\frac{\delta\mathcal{F}(\varphi; \langle\varphi\rangle)}{\delta\varphi} + [\Gamma(\varphi)]^{1/2}\xi(t) \quad (7)$$

and

$$\frac{\delta\mathcal{F}(\varphi; \langle\varphi\rangle)}{\delta\varphi} = [\varphi - K(\langle\varphi(t)\rangle - \varphi)]. \quad (8)$$

Note that  $\langle G(\varphi; \langle\varphi\rangle) \rangle = 0$  is the stationary state condition for the relaxational dynamics given by the globally coupled single-field problem. Moreover, if  $\omega=0$  then the system will reach a steady state since Eq. (3) becomes equivalent to Eq. (1). Without the contribution  $G$ , the set (6) describes a simple harmonic oscillator with frequency  $\omega$ .

We have been unable to solve these mean field equations analytically in spite of their apparent simplicity. The problem in applying existing methods for extended systems [12] lies in the difficulty in the evaluation of averaging integrals that have only been implemented for particular nonlinearities. Any attempt to approximate our relaxation function to achieve a tractable form misses the essential features of our problem and leads to a totally different behavior than that observed in the full problem. We can thus only describe the behavior on the basis of our numerical simulations.

We implement periodic boundary conditions in two-dimensional  $128 \times 128$  lattices, choosing parameter values which correspond to a point of multistability in Fig. 2. We focus on the case  $\sigma^2=3$  and  $\omega^2=0.1$ . Figure 3 shows  $\langle\varphi(t)\rangle$  vs  $\langle\dot{\varphi}(t)\rangle/\omega$  for two different sets of initial conditions indicated by arrows. For one set of initial conditions the system is driven toward the homogeneous state  $\langle\varphi(t)\rangle=\langle\dot{\varphi}(t)\rangle=0$ , while the other leads to an oscillatory regime. In the same figure we show the entire distribution of  $(\varphi_i(t), \dot{\varphi}_i(t)/\omega)$  at four different times during a period of oscillation once a stationary oscillatory regime is reached. It is interesting to note that, although some points fall within the attractor of the stable fixed point, they are, nevertheless, driven to the oscillatory orbit because they are driven by the average value and not by their individual dynamics.

In Fig. 4 we show spatial density plots for the values of  $\varphi_i(t)$  and  $\dot{\varphi}_i(t)/\omega$  at the centers of the clouds in Fig. 3. The oscillations of the field are represented by variations in time of the gray scale. Note the phase difference between the two fields. In Fig. 5 we show the time Fourier transform of the field average  $\langle\varphi(t)\rangle$  for the data shown in Fig. 3 for the case of the initial conditions leading to oscillatory behavior. The

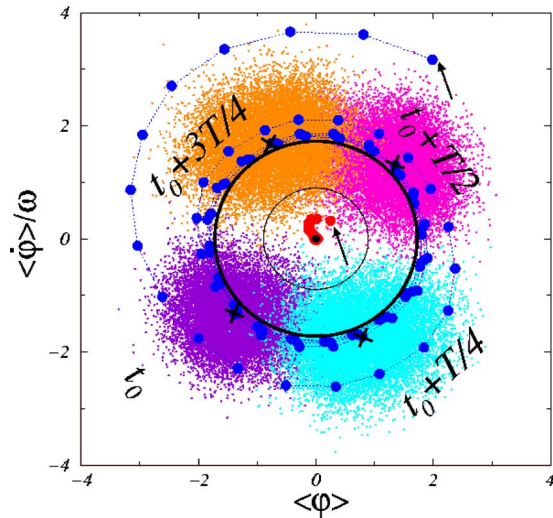


FIG. 3. (Color online) Simulation results:  $\langle\varphi(t)\rangle$  vs  $\langle\dot{\varphi}(t)\rangle/\omega$ . Depending on the initial conditions, the system ends in a homogeneous state or in a limit cycle. The central black dot indicates the stable fixed point. The wide solid black line is the stable limit cycle, and the thin black line the unstable limit cycle, obtained from Eq. (9). The numerical simulations for two sets of initial conditions indicated by arrows are plotted as a sequence of dots (blue and red, respectively, in color, gray in print). The clouds of points indicate the values of  $\varphi_i(t)$  and  $\dot{\varphi}_i(t)/\omega$  at four times that cover a period of oscillation once the oscillatory stationary regime is reached. The average values  $\langle\varphi(t)\rangle$  and  $\langle\dot{\varphi}(t)\rangle/\omega$  of these clouds are given by the circles (blue in color, gray in print) with a superimposed black cross.

system presents essentially the single frequency  $\omega$  in its dynamics.

We can summarize our broader observations based on numerical results as follows. Provided the noise intensity is not too much greater than the critical value for the single-field

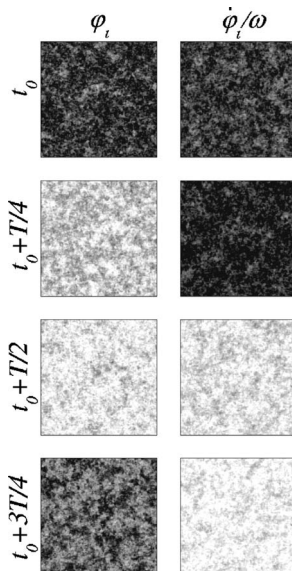


FIG. 4. Spatial density plots of  $\varphi_i$  and  $\dot{\varphi}_i/\omega$  at various times through a cycle for the clouds shown in Fig. 3. The gray scale is the same for all plots: black (-2) to white (+2). Note the oscillatory behavior and the phase difference between the two fields.

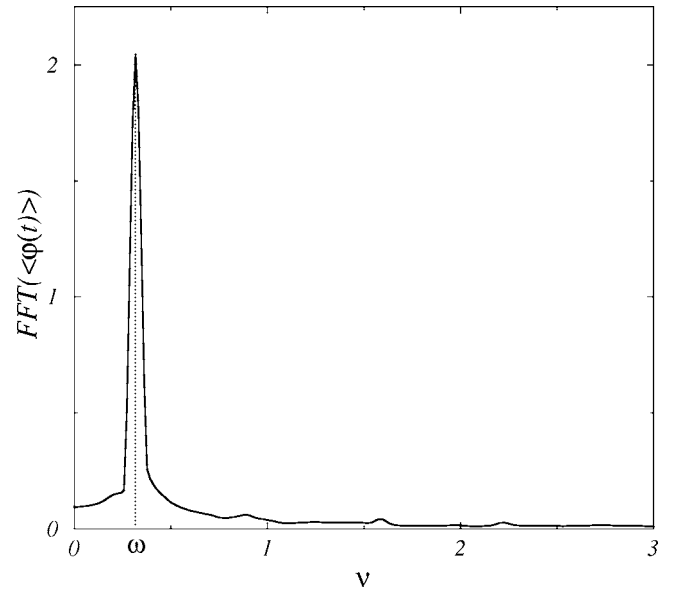


FIG. 5. Fourier transform of  $\langle\varphi(t)\rangle$  for the numerical simulations of Fig. 3 in the case of oscillatory asymptotic behavior.

problem, the mean values of the fields are well described by the simple forms

$$\langle\varphi(t)\rangle = \langle\varphi(t)\rangle_0 \cos(\omega t), \quad \langle z \rangle = \langle\varphi(t)\rangle_0 \sin(\omega t), \quad (9)$$

where  $\langle\varphi(t)\rangle_0$  is the mean value of the single-field problem. For simplicity, the initial phase has been set arbitrarily to zero. We thus find that the oscillations occur according to the harmonic nature of the problem in the absence of  $G$  in Eq. (6), with an amplitude determined by the relaxational dynamics in the absence of the oscillatory behavior. Thus, note again that in the absence of fluctuations no oscillatory behavior is obtained. Moreover, even if noise is present, the occurrence of collective oscillations depends on a sufficiently strong coupling. This then means that the trajectory in the space  $(\langle\varphi(t)\rangle, \langle\dot{\varphi}(t)\rangle/\omega)$  is a circle of radius  $\langle\varphi(t)\rangle_0$ . We also find that as the noise intensity increases, the trajectories remain periodic but that the circular shape becomes distorted so that there is an additional modulation of the amplitude.

A generalization of the relaxational model involves coupling terms that lead to morphological instabilities [8,10]. Instead of global order-disorder transitions, the model now leads to pattern formation. A prototypical example of this type of interaction is the so-called Swift-Hohenberg coupling, which in its continuous version reads  $\mathcal{L}_{SH} = -K(k_0^2 + \nabla^2)^2$ . The discretization of this operator is discussed in detail in [8,10], as is the mean field description that must now allow for possible spatial modulation of the solution. The structure of the mean amplitude problem turns out to be formally identical to that obtained for the mean field problem with diffusive coupling, as is the analytic characterization of the self-consistent solutions. The information provided by the solutions is of course different: in the case of diffusive coupling the ordered phases are global, whereas here they are patterned. The detailed structure of these patterns is discussed in [10].

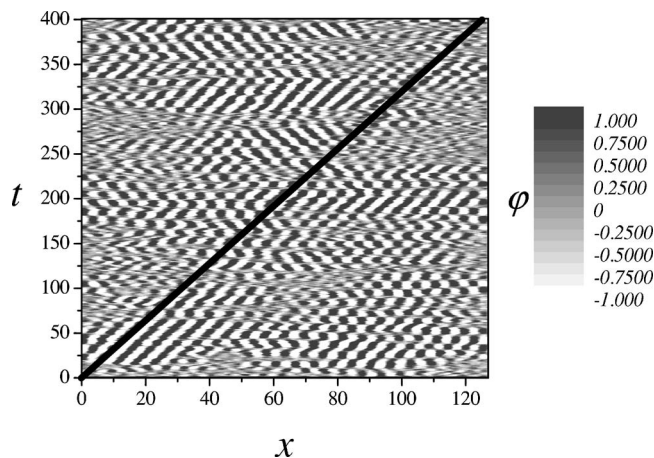


FIG. 6. Density plot for  $\varphi(x,t)$  obtained from a numerical simulation of Eq. (10) for a chain of 128 oscillators with periodic boundary conditions,  $K=10$ , and  $\sigma^2=3$ . The diagonal solid line has a slope  $\omega$ , and has been drawn to guide the eye. The spatial patterns are of length  $2\pi k^*$  with  $k^* \approx 1.05$ .

With a second degree of freedom, our extended system in one dimension (to which we restrict our numerical simulations) reads

$$\begin{aligned} \dot{\varphi}_i &= -\Gamma(\varphi) \left( \left[ 1 + K \left( 1 + 4 \sinh^2 \left( \frac{1}{2} \frac{\partial}{\partial x} \right) \right) \right] \varphi_i \right) \\ &\quad + [\Gamma(\varphi)]^{1/2} \xi_i(t) - \omega z_i, \\ \dot{z}_i &= \omega \varphi_i. \end{aligned} \quad (10)$$

The local potential is again harmonic. The particular form of the coupling operator arises from the discretization of the Swift-Hohenberg operator [8,10] and the choice  $k_0=1$ . We have carried out numerical simulations of Eq. (10) in a chain of  $N=128$  oscillators with periodic boundary conditions, with coupling coefficient  $K=10$  and noise intensity  $\sigma^2=3$ , which leads to an aspect ratio  $\Lambda \sim 20$  [10]. That is, at any given time, we expect approximately 20 wavelengths of the

pattern. Figure 6 shows  $\varphi(x,t)$  by means of a density plot. We find an oscillatory pattern with temporal and spatial modulations  $\omega$  and  $k^*$ , respectively ( $k^*$  is related to and close to  $k_0$ ; here  $k^* \approx 1.05$ , see [10]). For noise intensities near the critical value the fields are simply given by

$$\begin{aligned} \langle \varphi(x,t) \rangle &= 2\mathcal{A}(k^*) \cos(k^*x) \cos(\omega t), \\ \langle z(x,t) \rangle &= 2\mathcal{A}(k^*) \cos(k^*x) \sin(\omega t). \end{aligned} \quad (11)$$

Again for simplicity, we have set the spatial phase at the origin and the initial temporal phase to zero.

The phase diagram indicates that for the values of the parameters used in our simulation the system lies within a multistable region. We have explicitly shown this multistability in the single-field problem [10] and would expect that an oscillatory pattern develops or not depending on the initial condition. While certain regions in Fig. 6 appear less ordered than others and this might provide an indication of multistability, we did not pursue this possibility in detail, our purpose here being mainly to present the nature of the noise-induced spatio-temporal pattern.

Herein we have shown that in the presence of inertia in relaxational systems with field-dependent kinetic coefficients, noise may induce spatio-temporal oscillatory behavior in spatially extended systems. These systems are particularly interesting (and different from those in which transitions are induced dynamically [11]) because the transitions do not depend on the Stratonovich drift and thus occur regardless of the interpretation of the noise. We have supported our conclusions via numerical simulations. The challenge that remains is an analytic solution of the problem, even in the mean field case.

This work was partially supported by the National Science Foundation under Grant No. PHY-0354937 (K.L. and K.W.) and by the Ministerio de Educación y Ciencia (Spain) under Grant No. FIS2005-00457 (J.B.). J.B. gratefully acknowledges the *Ramón y Cajal* program that provides his researcher contract.

- 
- [1] P. C. Hohenberg and B. I. Halperin, *Rev. Mod. Phys.* **49**, 435 (1977).  
 [2] J. García-Ojalvo and J. M. Sancho, *Noise in Spatially Extended Systems* (Springer, New York, 1999).  
 [3] R. Montagne, E. Hernández-García, and M. San Miguel, *Physica D* **96**, 47 (1996).  
 [4] M. Ibañes, J. García-Ojalvo, R. Toral, and J. M. Sancho, *Phys. Rev. Lett.* **87**, 020601 (2001).  
 [5] H. L. Snyder, P. Meakin, and S. Reich, *Macromolecules* **16**, 757 (1983).  
 [6] C. Van den Broeck, J. M. R. Parrondo, and R. Toral, *Phys. Rev. Lett.* **73**, 3395 (1994); C. Van den Broeck, J. M. R. Parrondo, R. Toral, and R. Kawai, *Phys. Rev. E* **55**, 4084 (1997).  
 [7] O. Carrillo, M. Ibañes, J. García-Ojalvo, J. Casademunt, and J. M. Sancho, *Phys. Rev. E* **67**, 046110 (2003).  
 [8] J. Buceta, M. Ibañes, J. M. Sancho, and K. Lindenberg, *Phys. Rev. E* **67**, 021113 (2003).  
 [9] J. Buceta and K. Lindenberg, *Phys. Rev. E* **69**, 011102 (2004).  
 [10] K. Wood, J. Buceta, and K. Lindenberg, to appear in *Phys. Rev. E* **73**, 022101 (2006).  
 [11] R. Kawai, X. Sailer, L. Schimansky-Geier, and C. Van den Broeck, *Phys. Rev. E* **69**, 051104 (2004).  
 [12] R. Kuske, in *Nonlinear Stochastic Dynamics*, Solid Mechanics and Its Applications, edited by N. Sri Namachchivaya and Y. K. Lin (Kluwer, Dordrecht, 2003), Vol. 110; C. Mayol, R. Toral, and C. R. Mirasso, *Phys. Rev. E* **69**, 066141 (2004).